Title: RAPID AND LABEL-FREE DETECTION OF PROTEIN A BY APTAMER-TETHERED POROUS SILICON NANOSTRUCTURES

Authors: Katharina Urmann, Peggy Reich, Johanna-Gabriela Walter, Dieter Beckmann, Ester Segal, Thomas Scheper

PII: S0168-1656(17)30022-6
DOI: http://dx.doi.org/doi:10.1016/j.jbiotec.2017.01.005
Reference: BIOTEC 7766

To appear in: *Journal of Biotechnology*

Received date: 13-9-2016
Revised date: 19-1-2017
Accepted date: 24-1-2017

Please cite this article as: Urmann, Katharina, Reich, Peggy, Walter, Johanna-Gabriela, Beckmann, Dieter, Segal, Ester, Scheper, Thomas, RAPID AND LABEL-FREE DETECTION OF PROTEIN A BY APTAMER-TETHERED POROUS SILICON NANOSTRUCTURES.Journal of Biotechnology http://dx.doi.org/10.1016/j.jbiotec.2017.01.005

RAPID AND LABEL-FREE DETECTION OF PROTEIN A BY APTAMER-TETHERED POROUS SILICON NANOSTRUCTURES

Katharina Urmann[a,b,‡], *Peggy Reich*[a,c,‡], *Johanna-Gabriela Walter*[a], *Dieter Beckmann*[c], *Ester Segal*[b]*, *Thomas Scheper*[a]*

‡ Equal contribution, * Corresponding authors

[a] Institute of Technical Chemistry, Leibniz Universität Hannover, Callinstr. 5, 30167 Hanover, Germany; phone: +49-511-7622269; e-mail: scheper@iftc.uni-hannover.de

[b] Department of Biotechnology and Food Engineering, Technion Israel Institute of Technology, Technion City, 32000 Haifa, Israel; phone: +972-4-8295071; e-mail: esegal@technion.ac.il

[c] Institute for Bioprocessing and Analytical Measurement Techniques e.V., Rosenhof, 37308 Heilbad Heiligenstadt, Germany

KEYWORDS

Optical Biosensor, Aptamer, Porous Silicon, Label-Free, Protein A, *Staphylococcus aureus*

Graphical abstract

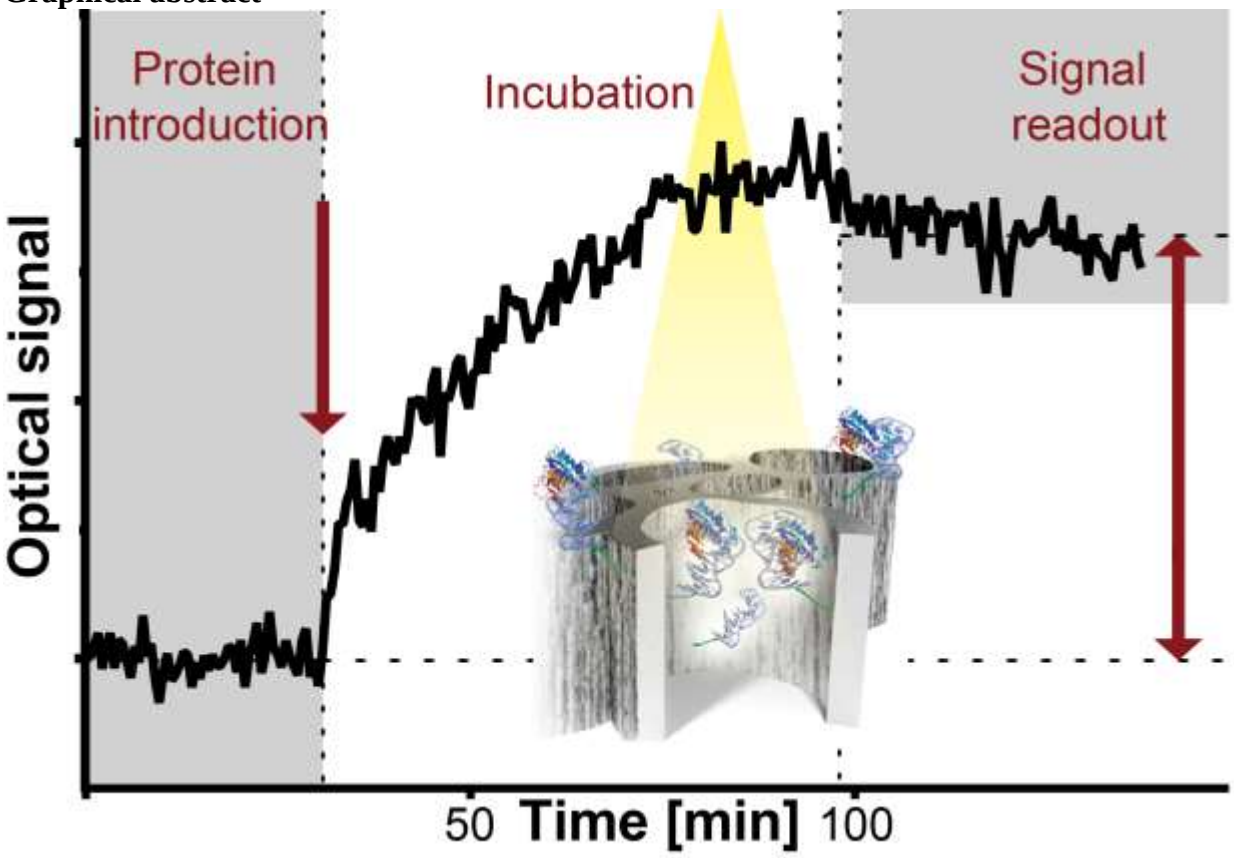

HIGHLIGHTS

- Aptamer-conjugated porous Si nanostructures are designed as optical biosensors
- Selective detection and quantification of the target analyte protein A is demonstrated
- A sandwich assay format is demonstrated for signal enhancement
- The biosensor allows rapid, label-free and simple analysis

ABSTRACT

Protein A, which is secreted by and displayed on the cell membrane of *Staphylococcus aureus* is an important biomarker for *S. aureus*. Thus, its rapid and specific detection may facilitate the pathogen identification and initiation of proper treatment. Herein, we present a simple, label-free and rapid optical biosensor enabling specific detection of protein A. Protein A-binding aptamer serves as the capture probe and is immobilized onto a nanostructured porous silicon thin film, which serves as the optical transducer element. We demonstrate high sensitivity of the biosensor with a linear detection range between 8-23 μM. The apparent dissociation constant was determined as 13.98 μM and the LoD is 3.17 μM. Harnessing the affinity between protein A and antibodies, a sandwich assay format was developed to amplify the optical signal associated with protein A capture by the aptamer. Using this approach, we increase the sensitivity of the biosensor, resulting in a three times lower LoD.

1. INTRODUCTION

Staphylococcus aureus is a leading cause of infections and bacteremia in humans, but also causing food-borne diseases due to excretion of several enterotoxins [1]. Treatment is especially challenging as *S. aureus* has a remarkable ability to rapidly adapt its genetic characteristics and develop resistance against new antibiotics [2,3]. Hence, the most efficient way to fight *S. aureus* infections is to prevent their transmission by isolation, decontamination and strict hygienic guidelines. Moreover, studies have concluded that active screening for methicillin-resistant *Staphylococcus aureus* (MRSA) can efficiently reduce bloodstream infections, which results in high mortality [4,5].

Rapid and reliable detection and identification of MRSA is critical for effective infection control as well as for therapeutic decisions. Traditional culturing techniques using selective media are sensitive and cost-effective, but are time-consuming (several days) and therefore problematic [6,7]. Molecular methods based on polymerase chain reaction (PCR) exhibit faster turnaround times (~2-6 h) and are considered the gold standard for MRSA detection nowadays; however, they are cost-intense, require trained staff and may not keep up with new evolving genetic variants [8]. A rapid user-friendly point-of-care test for *S. aureus* is thus urgently needed to allow fast screening of patient samples and provide effective infection control.

Protein A, a virulence factor specific for *S. aureus*, is linked to peptidoglycans on the bacterial cell surface and promotes general surface adhesion [9]. Protein A binds to the von Willebrand factor (vWF), an essential protein for hemostasis, and therefore promotes wound infection. It also binds the Fc-region of human antibodies, thereby inhibiting phagocytosis, which in consequence prevents bacterial elimination [10,11]. Real-time PCR for typing and detection of different *S. aureus* variants utilizes the specific spa gene, encoding protein A. As the gene is

highly conserved, showing one mutation in 70 months [12], protein A provides an optimal molecular marker for the detection of *S. aureus*. Several assays, mostly ELISA (Enzyme Linked Immunosorbent Assay) based, for the detection of protein A using antibodies have been developed [13] and are commercially available. While these labeled techniques are highly sensitive, they suffer from several limitations, which are ascribed to the complicated required equipment and the delicate nature of the antibody receptor and its costs [14,15].

Aptamers are single-stranded DNA or RNA oligonucleotides with the ability to specifically bind their target due to their unique 3-dimensional structure. Aptamers are selected *in vitro* for a specific target using the Systematic Evolution of Ligands by Exponential Enrichment (SELEX) process [16]. Aptamers can be engineered towards specific targets, ranging from small molecules or proteins to whole cells, and synthesized with high reproducibility and at a fraction of the cost of antibodies [14,17,18]. Thus, due to these advantageous properties, a variety of aptamer-based analytical methods and biosensors have been developed in recent years, also for the detection of *S. aureus* [19-22]. Lian et al. developed a piezoelectric sensor employing *S. aureus* aptamer and demonstrated detection at bacterial concentrations as low as 59 CFU/mL in milk samples [23]. The aptamer they used was selected against *S. aureus* whole cells and as such, the molecular binding site of the aptamer on the cell surface is unknown [24]. Since *S. aureus* has many variants and is evolving quickly, the aptamer may lose its affinity, thereby limiting the applicability of this method [12].

Recently, the Strehlitz group has developed a modified SELEX process, termed FluMag-SELEX, wherein the target is immobilized on magnetic beads and fluorescent labels are used for aptamer quantification [25]. Using this process, they selected an aptamer binding protein A with high

affinity and demonstrated that it binds specifically to both, native and recombinant protein A, but not to other immunoglobulin-binding proteins like protein G.

Herein, we use this aptamer as a receptor for the design of a label-free optical biosensor. The biosensor is based on a porous silicon (PSi) nanostructure which is used as the optical transducer. PSi-based optical biosensors have demonstrated outstanding performance in terms of rapid and reliable detection of numerous targets [26-29]. Specifically, biosensors employing interferometric Fourier transform spectroscopy (RIFTS) [30-32], which harness the series of Fabry-Pérot interference fringes from light reflections from the top and bottom interfaces of a porous thin film, allow for the design of simple and sensitive detection of a specific analyte upon its binding to surface-tethered capture probes [33-35]. Recently, the excellent integration of aptamers as capture probes with PSi-based transducers has been demonstrated, enabling exceptionally stable and reliable biosensing, applicable for both, proteins and bacteria [36-39].

In the present study, protein A-targeting aptamers are conjugated to PSi thin films and the resulting biosensors demonstrate a specific detection and quantification of protein A in a range of 2 to 50 µM with a total assay time of < 2 h. The biosensing scheme is further optimized and we show a measured limit of detection (LoD) of 1 µM.

2. MATERIAL AND METHODS

2.1 Materials

Heavily boron doped p-type Si wafers (0.0008 Ω·cm resistivity, <100>-oriented) were purchased from Sil'tronix Silicon Technologies (France). Aqueous HF (48%) and ethanol absolute were obtained from Merck and toluene and acetone were supplied by Gadot Biochemical Industries LTD (Israel). (3-aminopropyl)-triethoxysilane (APTES), succinic acid, *N*-(3-

Dimethylaminopropyl)-*N*-ethylcarbodiimide hydrochloride (EDC) and all buffer salts were purchased from Sigma-Aldrich Chemicals. Buffers were prepared with deionized water (18.2 MΩ cm), filtered and autoclaved prior to use. The protein A-binding aptamer, selected by Stoltenburg et al. [40] was used in its truncated form PA#2/8[S1-58]: 5'- ATA CCA GCT TAT TCA ATT AGC AAC ATG AGG GGG ATA GAG GGG GTG GGT TCT CTC GGC T -3'(abbreviated as PAA). Its selection buffer (SB) was composed of 20 mM Tris base (Trizma, Sigma Aldrich), 100 mM NaCl, 5 mM KCl, 10 mM $MgCl_2$, and 1 mM $CaCl_2$. MES buffer was composed of 100 mM 2-Morpholinoethanesulfonic acid at pH 6. PAA and a completely randomized 40 nucleotides long DNA-Pool (N_{40}) were purchased with a 3'-amino-C6-modification from Integrated DNA Technologies (Coralville, USA). Biosensing experiments were performed with the following proteins: recombinant protein A (PA) and IgG from human serum (both from Sigma-Aldrich Chemicals). As Tween 20 enhances protein solubility, all proteins solutions were prepared in SB supplemented with 0.005% Tween 20 (SBT).

2.2 Preparation of Oxidized PSi

Si wafers were anodized in a two-step process. First, a sacrificial layer was etched at a constant current density of 375 mA/cm^2 for 30 s in a solution of 3:1 (v/v) aqueous HF (48%) and ethanol. Etching setup details are reported elsewhere [30,41]. The resulting PSi layer was dissolved in an aqueous NaOH solution (0.1 M). Next, a second etching step was performed using the above-mentioned conditions. After each step, the silicon surface was thoroughly rinsed with ethanol and dried under a stream of nitrogen. Finally, the PSi samples were thermally oxidized in a tube furnace (Thermolyne) at 800 °C for 1 h in ambient air, yielding oxidized PSi ($PSiO_2$) scaffolds.

2.3 Characterization of $PSiO_2$ Films

The nanostructure and the thickness of the neat $PSiO_2$ samples were studied by a Carl Zeiss Ultra Plus high-resolution scanning electron microscopy (HRSEM) at an accelerating voltage of 1 keV. The porosity of the films was characterized by gravimetry (for porosity), and the spectroscopic liquid infiltration method (SLIM) [30], as described by Massad-Ivanir *et al.* [42].

2.4 Aptamer Immobilization onto $PSiO_2$ Films

The aptamer was conjugated to the $PSiO_2$ films by a previously described coupling chemistry [36]. Briefly, the $PSiO_2$ was amino-modified by incubation (1 h) in a solution of APTES in toluene (42 mM); after which, the samples were rinsed with toluene, ethanol and acetone and dried under a nitrogen stream. Next, the $PSiO_2$ was incubated for 30 min in a freshly prepared solution of 100 mg succinic acid in 4.7 mL DMSO (dimethyl sulfoxide) and 300 µL of 0.1 M $NaHCO_3$, pH 9.4 and subsequently washed with DMSO and deionized water. Successive chemical modifications were carried out in a custom made Plexiglas flow cell [36]. A 52 mM solution of EDC in MES was introduced into the flow cell and allowed to react for 1 h. Next, 50 µL of the aptamer solution (75 µM in MES) was introduced and incubated with the surface for 1 h, followed by washing with 10 mL MES. Finally, the surface was incubated for 30 min with 300 µL of 0.1 M ethanolamine solution to block remaining active sites.

2.5 Infrared Spectroscopy

Surface modification steps were followed with attenuated total reflectance Fourier transform infrared (ATR-FTIR) spectroscopy. Spectra were recorded using a Thermo 6700 FTIR instrument equipped with a Smart iTR diamond ATR device.

2.6 Measurement of Interferometric Reflectance Spectra and Protein Biosensing

The experimental setup for optical measurements and biosensing experiments is schematically illustrated in Figure 1A. The sample was mounted in a fixed flow cell to ensure that data is

collected from the same spot during the entire course of measurements. Reflectivity spectra were collected by an Ocean Optics charge-coupled device (CCD) USB 4000 spectrometer coupled to a microscope objective lens with a bifurcated fiber-optic cable. A tungsten light source was connected to the second port of the fiber-optic cable and the light spot was focused onto the center of the $PSiO_2$ sample (spot size 1-2 mm^2). Surface illumination and detection of the reflected light were both performed along an axis coincident with the surface normal. Spectra were continuously recorded every 30 s at a spectral acquisition time of 100 ms and in the wavelength range of 400-1000 nm. The raw spectra (see Fig. 1B-1) were processed in real time by applying Fast Fourier Transformation (FFT). The FFT spectra, shown in Fig. 1B-2, depict a single peak, whose location along the x-axis corresponds to the effective optical thickness (EOT) of the film. The latter equals 2nL, where n is the effective refractive index and L is the physical thickness of the porous film.

Prior to biosensing experiments, the PAA-modified $PSiO_2$ were rinsed with boiling deionized water to unfold any secondary structures in the oligonucleotide and followed by incubation in SB to allow functional folding of the aptamer. In a typical biosensing experiment, a baseline was recorded in SB followed by introduction of the protein dissolved in SBT (100 µL) and incubation for 1 h. Next, the protein solution was removed and the biosensor was rinsed extensively with SB (10 mL). Reflectivity spectra were recorded every 30 s throughout the entire experiment and data are presented as the relative change of EOT in respect to a baseline value (as depicted in Fig. 1B-3). Please note that during buffer exchange and rinsing steps, EOT measurements were shortly paused to allow a thorough washing of the biosensor and the flow cell.

2.7 Statistical and regression analysis

For statistical analysis, unpaired t-tests were performed. Resulting two-tailed P values below 0.05 were required to consider the compared groups as significantly different from each other. Non-linear regressions were performed using SigmaPlot software (Systat Software, Inc).

3. RESULTS AND DISCUSSION

3.1 Functionalization of $PSiO_2$ Films with Amino-Modified Aptamers

Porous silicon thin films were prepared from heavily boron-doped p-type crystalline Si wafers by anodization at a constant current of 375 mA/cm^2 for 30 s. In order to stabilize the PSi nanostructure and to render it more hydrophilic, the films were thermally oxidized for 1 h at 800 °C [43]. The thickness of the resulting films, as determined from HRSEM studies, is ~5500 nm and their morphology (see Fig. 1A, bottom panel) is characterized by interconnected cylindrical pores with pore size ranging between 35 and 65 nm. The porosity of the films is 70%, calculated based on SLIM and gravimetry experiments (data not shown). Thus, the film's nanostructure provides a high surface area and large porous volume for proper infiltration of biomolecules (e.g., the diameter of PA is approximately 5.3 nm, based on the number of amino acid residues [44]) and their interaction.

Previous studies by Stoltenburg et al. [40] have shown that the protein A-binding aptamers (PAA) possess higher functionality when immobilized from the 3' terminus, hence, we have used 3'-amino modified aptamers. The latter were conjugated to the $PSiO_2$ by standard carbodiimide-mediated coupling chemistry [36]. Preferably, the aptamer immobilization should be carried out in its selection buffer (SB) [45]. However, as in this case the aptamer's SB contains Tris, which could impede its conjugation to the $PSiO_2$ surface, immobilization was carried out in MES buffer instead. $PSiO_2$ surface modifications and aptamer-conjugation were verified by ATR-FTIR (see

Fig. S1, SI) and were found to coincide with our previous work [36,37]. As the aptamers' ability to bind their targets depends crucially on proper folding and 3-D structure [46,47], the aptamer-modified $PSiO_2$ films were thermally treated at 100°C (well above the predicted melting temperature of the aptamer [48]) in order to allow the PAA to unfold. To support the tethered aptamers to correctly fold into their functional structure, the porous films were incubated in SB prior to subsequent biosensing experiments.

3.2 Optical Biosensing Experiments with Protein A

PAA-modified $PSiO_2$ films were exposed to different concentrations of PA solutions to investigate the target-aptamer binding behavior within the nanoporous scaffold. In a typical biosensing experiment, the reflectivity spectra of the biosensors were monitored in real time and corresponding EOT values were computed. Figure 2 presents the change in the relative EOT ($\Delta EOT/EOT_0$) upon exposure of the biosensor to recombinant PA from *S. aureus* (molecular weight 45 kDa) at a concentration of 5 µM. First, SB buffer was introduced into the flow cell to acquire a stable EOT baseline. Subsequently, the target solution was injected and incubated with the aptamer-conjugated $PSiO_2$. Immediately after the introduction of PA, a rapid increase in the relative EOT value is observed, after which the signal steadily increases until a constant EOT value was attained (after ~ 1 h). This represents a typical binding curve: PA infiltrates into the pores and is bound by PAA inducing an increase in the EOT. Thereafter, the protein solution was removed and the biosensor surface was extensively rinsed with SB to eliminate unbound protein molecules and attaining a new stable EOT value. The avaeraged optical signal, expressed as the relative change in EOT, for a concentration of 5 µM PA was 1.46 ± 0.27 ($\Delta EOT/EOT_0 \times 10^3$) on

average. In a control experiment (see Fig. 2, trace b), the biosensor was exposed to a non-target protein, human IgG (molecular weight 150 kDa) at the same concentration (5 µM). The EOT is observed to rapidly increase upon the IgG introduction due to the higher refractive index of this solution. During incubation, minor changes in the EOT occur, possibly owing to unspecific adsorption of IgG to the porous scaffold.

3.3 Non-specific Adsorption and Aptamer Selectivity

Next, control experiments were performed utilizing an amino-modified DNA-Pool, investigating non-specific adsorption and verifying aptamer selectivity. In these experiments, random sequence oligonucleotides (40-bases long, N_{40}) were immobilized onto $PSiO_2$ in the same manner and concentration as previously described for PAA and biosensing experiments were performed by exposing the N_{40}-functionalized $PSiO_2$ to IgG (5 µM). Figure 3 summarizes results of these experiments and presents the average relative change in EOT in comparison to values obtained for the PAA-functionalized biosensors upon exposure to IgG and the target PA (at a concentration of 5 µM). Both, the N_{40}-and the PAA-functionalized $PSiO_2$, exhibit comparable relative EOT changes (of 0.92 ± 0.09 and 0.85 ± 0.16 respectively) upon incubation with the IgG solution. These results suggest that the increase in EOT can be attributed to non-specific adsorption of IgG onto the porous surface and not to binding by the aptamers. Whereas, the PAA-functionalized biosensors are exposed to the PA, the attained EOT change is considerably higher (by 62 %) and these are statistically significant. Moreover, it is important to note that IgG molecules are more than 3 times larger (molecular weight 150 kDa) than PA (45 kDa) and thus, a smaller number of IgG molecules can evoke a higher optical signal. Hence, the biosensor response upon exposure to IgG is not only significantly lower in signal, but is also expected to

represent the adsorption of much fewer IgG molecules in comparison to the specific binding of PA.

3.4 Binding Affinity Characterization

To determine the binding affinity, the PAA-functionalized $PSiO_2$ biosensor responses from different concentrations of PA and IgG were analyzed. Figure 4 shows the biosensor response, expressed as the relative EOT change, for different PA concentrations. The sensor response shows a consistent behavior and the relative EOT change increases with increasing concentration of PA. The data were fit to the three-parameters Hill function (see Equation 1) [49] presented as the solid black line in Figure 4.

$$R = R_{max}\frac{[T]^h}{K_{0.5}+[T]^h} \qquad \text{Equation 1}$$

where R is the relative change in EOT of the biosensor to the target concentration [T], R_{max} is the maximal response signal at $[T] \rightarrow \infty$, h the Hill coefficient and $K_{0.5}$ the equilibrium constant, also known as the apparent dissociation constant K_D.

The three-parameter Hill function is a suitable model to describe biosensor characteristics from its binding curve as shown by Kurganov et al. [50]. The equilibrium constant $K_{0.5}$ (K_D) is calculated to be 14 ± 1 µM, describing the concentration at which half of the maximum signal is attained. For [T] → ∞, saturation of the biosensor occurs at a relative EOT change of 10.1 ± 0.9, corresponding to R_{max}. The sensitivity, S, of a biosensor is defined as $S = \frac{\Delta R}{\Delta[T]}$, expressing the ratio of signal change ΔR per concentration change Δ[T]. Accordingly, the sensitivity of PAA-functionalized $PSiO_2$ biosensors is determined as the slope at $K_{0.5}$ and is 0.6 (in ($\Delta EOT/EOT_0$ x 10^3)/µM), implying that the optical signal increases by ~0.6 per µM of the target PA. The Hill

coefficient h represents an "interaction coefficient", and in case of a very strong positive cooperativity it reflects the stochiometry of binding. In this case, the calculated value of 2.6 ± 0.7 indicates multiple binding between every PA molecule and aptamers immobilized within the $PSiO_2$ nanostructure (PA exhibits 5 identicalbinding sites [51]). The correlation coefficient R^2 is 0.977, proving excellent prediction of the experimental data using this model.

It should be noted that that the K_D value obtained in this work varies from that calculated by Stoltenburg et al. [40]. The apparent K_D is known to be highly depending on the method of the affinity characterization [52]. Hence, different values for PAA affinity have been reported for measurements with either microscale thermophoresis or surface Plasmon resonance [40]. The main reason for the differences may lie in the accessibility of the aptamer binding sites due to its immobilization on a surface [53]. Recent studies by Chang et al. [54,55], comparing between literature-reported K_D values and their obtained results, highlighted that differences in K_Ds are largely attributed to the effect of environmental and experimental conditions on aptamer binding kinetics and affinities.

3.4 Limit of Detection

The limit of detection (LoD) for the presented aptamer-based optical $PSiO_2$ biosensor was determined from the standard deviation of the relative EOT. Standard deviation between relative EOT values (measured during baseline establishment and incubation of the biosensors in SB) was calculated to be σ= 0.068 (as $\Delta EOT/EOT_0$ x10^3). By definition, the LoD corresponds to a protein concentration which can be reliably distinguished from the background noise. With a confidence level of 99.7% this is true for an optical signal as high as $3*\sigma$ = 0.205 (as

$\Delta EOT/EOT_0$ x10^3). Thus, by interpolation of the Hill fit (see Fig. 4), the LoD was determined as 3.166 µM.

The resolution of a sensor is defined as the smallest change in analyte concentration that can be detected, $Res = \frac{noise}{S}$. With the previously calculated biosensor sensitivity S and obtained background noise, the resolution was calculated as 0.113 µM for the PAA modified scaffold. The errors for both LoD and sensitivity can be approximated by error propagation [56] of the previously obtained Hill equation under the assumption that all variables are independent from each other (LoD = 3.17 µM ± 1.29; Res = 0.11 µM ± 0.02). It should be emphasized that the LoD and the resolution are instrument-specific and in this case, it is assumed that the instrument is the limiting factor. While aptamer-based protein A detection has been previously reported with a higher affinity value (K_D = 287 ± 16 nM) [40] and thus a lower LoD, the inherently high standard deviation of RIFTS signals is accredited to the simplicity of the experimental setup. However, there are possibilities to lower the noise, e.g. by minimizing environmental influences (i.e. temperature) or by means of signal processing [57].

3.5 Enhancing the Biosensor Sensitivity: Sandwich Assay with IgG

Finally, we present a sandwich assay designed for the enhancement of optical signals induced by PA binding to the surface-tethered PAA within the nanostructured PSi films. For this assay, it is assumed that PA binds to the PAA-functionalized $PSiO_2$ biosensor even at low concentrations, however, the number of molecules being too low to cause a change in EOT above the noise level. Protein A is known for its affinity to the Fc-region of antibodies and often used for their oriented immobilization in order to retain their ability to bind their specific antigen [10,58-60]. Furthermore, it is known, that protein A has five IgG binding domains [51]. Thus, introduction of

IgG should result in its binding by the aptamer-captured PA. As the molecular weight of IgG is three times larger than that of PA, a distinct change in EOT is expected even when the number of molecule is low. Figure 5 presents the change of relative EOT over time for a characteristic experiment in which we study the response of the biosensors to a PA concentration of 1 µM, which is well below the calculated LoD. Upon introduction of PA, no significant change in the EOT can be observed. Subsequent injection of IgG at the same low concentration (1 µM) induces a rapid response, depicting a typical binding behavior (see Fig. 5a). For comparison, Figure 5b shows the EOT signal of the biosensor to IgG exposure, while eliminating/ prior introduction to PA. In this case, a negligible change in the EOT is detected following the rinsing step, indicating that no specific binding has occurred.

Figure 6 summarizes the results of the developed sandwich assay. While the biosensing signals from a single exposure to either PA or IgG were insignificant and below the critical value ($3*\sigma = 0.205$) calculated for the LoD, the values atteined by the sandwich assay were six times higher (1.2 ± 0.3 as $\Delta EOT/EOT_0 \times 10^3$). Thus, the sandwich assay results in an experimental LoD value of 1 µM. While signal amplification in the presented sandwich assay relies on the specific binding between PA and antibody, this approach can certainly be applied to other biosensors. Most protein ligands have more than one binding site for aptamers or antibodies and can thus be exposed to a secondary ligand for signal amplification.

4. CONCLUSIONS

Reliable and fast detection of protein A is an important step towards improved diagnosis of *S. aureus* infections. Since direct recognition of *S. aureus* bacteria cells is hampered by the fast

evolution of the bacterial genome, capture of the highly conserved protein A, expressed by 99% of *S. aureus* strains [61], may provide indirect detection of *S. aureus*. Even though a demanded LoD for the clinical detection of protein A has not been established yet, protein A-targeting aptamers have already proven to be suitable capture probes, convincing with their high selectivity, sensitivity and superior stability. Herein, PAA was successfully integrated into a simple optical biosensor scheme based on a nanostructured PSi. The biosensor displays a high sensitivity with a ten-fold higher change in the EOT signal (6%; 0.6 as $\Delta EOT/EOT_0$ $x10^3$) per µM protein A than the noise (0.7%; 0.068 as $\Delta EOT/EOT_0$ $x10^3$) in a linear range of the target concentration (8-23 µM). Its binding affinity towards protein A is determined to be 13.98 µM with an LoD value of 3.17 µM. Taking advantage of the affinity between protein A and antibodies, we demonstrate a proof-of-concept scheme for enhancing the sensitivity of the PAA-functionalized $PSiO_2$ biosensors by three fold. Subsequent introduction of IgG in a sandwich-assay format allows for the detection of protein A at a concentration of 1 µM. Due to the severity of *S. aureus* infections, for cleinical applications, every cell and therefore all secreted protein A should be detected. Thus, further work should be directed towards lowering the limit of detection and increasing the dynamic range of the biosensor, however, we believe that the short assay time combined with the simplicity of the system can provide a suitable point-of-care method for fast identification of *S. aureus* infections in future clinical application.

ACKNOWLEDGMENT

This work was funded by the German Research Foundation under the grant SCHE 279/32-1. ES acknowledges the support by the Israel Science Foundation (Grant 1146/12). ES and KU acknowledge the core services and support from the Lorry I. Lokey Center for Life Science and

Engineering. PR acknowledges the financial support of the Life Science Network stipend, administered by the German Technion Society.

REFERENCES

1. Foster TJ, Geoghegan JA, Schwartzman Y-WTSLP. Chapter 37 - Staphylococcus aureus. *Molecular Medical Microbiology (Second Edition)*. Boston: Academic Press; 2015:655-674.
2. Maple PAC, Hamilton-Miller JMT, Brumfitt W. Originally published as Volume 1, Issue 8637WORLD-WIDE ANTIBIOTIC RESISTANCE IN METHICILLIN-RESISTANT STAPHYLOCOCCUS AUREUS. *The Lancet.* 1989/03/11 1989;333(8637):537-540.
3. Chambers HF, DeLeo FR. Waves of Resistance: Staphylococcus aureus in the Antibiotic Era. *Nature reviews. Microbiology.* 2009;7(9):629-641.
4. Tacconelli E, De Angelis G, de Waure C, Cataldo MA, Torre GL, Cauda R. Rapid screening tests for meticillin-resistant Staphylococcus aureus at hospital admission: systematic review and meta-analysis. *The Lancet Infectious Diseases.* 9// 2009;9(9):546-554.
5. Pronovost P, Needham D, Berenholtz S, et al. An Intervention to Decrease Catheter-Related Bloodstream Infections in the ICU. *New England Journal of Medicine.* 2006;355(26):2725-2732.
6. Lee BY, Singh A, David MZ, et al. The economic burden of community-associated methicillin-resistant Staphylococcus aureus (CA-MRSA). *Clinical Microbiology and Infection.* 6// 2013;19(6):528-536.
7. Francois P, Pittet D, Bento M, et al. Rapid Detection of Methicillin-Resistant Staphylococcus aureus Directly from Sterile or Nonsterile Clinical Samples by a New Molecular Assay. *Journal of Clinical Microbiology.* January 1, 2003 2003;41(1):254-260.
8. Kluytmans J. Control of meticillin-resistant Staphylococcus aureus (MRSA) and the value of rapid tests. *Journal of Hospital Infection.*65:100-104.
9. DeDent AC, McAdow M, Schneewind O. Distribution of Protein A on the Surface of Staphylococcus aureus. *Journal of Bacteriology.* June 15, 2007 2007;189(12):4473-4484.
10. Hartleib J, Köhler N, Dickinson RB, et al. Protein A is the von Willebrand factor binding protein on Staphylococcus aureus. *Blood.* 2000-09-15 00:00:00 2000;96(6):2149-2156.
11. Kim HK, Emolo C, DeDent AC, Falugi F, Missiakas DM, Schneewind O. Protein A-specific monoclonal antibodies and prevention of Staphylococcus aureus disease in mice. *Infect Immun.* Oct 2012;80(10):3460-3470.
12. Kahl BC, Mellmann A, Deiwick S, Peters G, Harmsen D. Variation of the Polymorphic Region X of the Protein A Gene during Persistent Airway Infection of Cystic Fibrosis Patients Reflects Two Independent Mechanisms of Genetic Change in Staphylococcus aureus. *Journal of Clinical Microbiology.* 2005;43(1):502-505.
13. Hsin Chang Y, Chang TC, Kao EF, Chou C. Detection of Protein A Produced by Staphylococcus aureus with a Fiber-optic-based Biosensor. *Bioscience, Biotechnology, and Biochemistry.* 2014/07/30 1996;60(10):1571-1574.
14. Song K-M, Lee S, Ban C. Aptamers and Their Biological Applications. *Sensors (Basel, Switzerland).* 01/0911/29/received12/31/revised01/04/accepted 2012;12(1):612-631.

15. Lakhin AV, Tarantul VZ, Gening LV. Aptamers: Problems, Solutions and Prospects. *Acta Naturae.* Oct-Dec 2013;5(4):34-43.
16. Tuerk C, Gold L. Systematic evolution of ligands by exponential enrichment: RNA ligands to bacteriophage T4 DNA polymerase. *Science (New York, N.Y.).* Aug 3 1990;249(4968):505-510.
17. Bunka DHJ, Stockley PG. Aptamers come of age - at last. *Nat. Rev. Microbiol.* Aug 2006;4(8):588-596.
18. Strehlitz B, Nikolaus N, Stoltenburg R. Protein detection with aptamer biosensors. *Sensors.* Jul 2008;8(7):4296-4307.
19. Yuan J, Wu S, Duan N, et al. A sensitive gold nanoparticle-based colorimetric aptasensor for Staphylococcus aureus. *Talanta.* 9/1/ 2014;127:163-168.
20. Duan N, Wu S, Zhu C, et al. Dual-color upconversion fluorescence and aptamer-functionalized magnetic nanoparticles-based bioassay for the simultaneous detection of Salmonella Typhimurium and Staphylococcus aureus. *Analytica Chimica Acta.* 4/20/ 2012;723:1-6.
21. Jia F, Duan N, Wu S, et al. Impedimetric aptasensor for Staphylococcus aureus based on nanocomposite prepared from reduced graphene oxide and gold nanoparticles. *Microchimica Acta.* 2014;181(9):967-974.
22. Baumstummler A, Lehmann D, Janjic N, Ochsner UA. Specific capture and detection of Staphylococcus aureus with high-affinity modified aptamers to cell surface components. *Letters in applied microbiology.* Oct 2014;59(4):422-431.
23. Lian Y, He F, Wang H, Tong F. A new aptamer/graphene interdigitated gold electrode piezoelectric sensor for rapid and specific detection of Staphylococcus aureus. *Biosensors and Bioelectronics.* 2015;65:314-319.
24. Shangguan D, Bing T, Zhang N. Cell-SELEX: Aptamer Selection Against Whole Cells. In: Tan W, Fang X, eds. *Aptamers Selected by Cell-SELEX for Theranostics*. Berlin, Heidelberg: Springer Berlin Heidelberg; 2015:13-33.
25. Stoltenburg R, Reinemann C, Strehlitz B. FluMag-SELEX as an advantageous method for DNA aptamer selection. *Analytical and Bioanalytical Chemistry.* 2005;383(1):83-91.
26. Massad-Ivanir N, Shtenberg G, Tzur A, Krepker MA, Segal E. Engineering Nanostructured Porous SiO2 Surfaces for Bacteria Detection via "Direct Cell Capture". *Analytical Chemistry.* 2011/05/01 2011;83(9):3282-3289.
27. Dancil KPS, Greiner DP, Sailor MJ. A porous silicon optical biosensor: Detection of reversible binding of IgG to a protein A-modified surface. *Journal of the American Chemical Society.* Sep 1999;121(34):7925-7930.
28. Bonanno LM, DeLouise LA. Whole blood optical biosensor. *Biosensors and Bioelectronics.* Oct 31 2007;23(3):444-448.
29. Beavers KR, Mares JW, Swartz CM, Zhao Y, Weiss SM, Duvall CL. In Situ Synthesis of Peptide Nucleic Acids in Porous Silicon for Drug Delivery and Biosensing. *Bioconjugate Chemistry.* 06/2003/16/received06/01/revised 2014;25(7):1192-1197.
30. Sailor MJ. *Porous silicon in practice: preparation, characterization and applications*: John Wiley & Sons; 2012.
31. Pacholski C, Yu C, Miskelly GM, Godin D, Sailor MJ. Reflective Interferometric Fourier Transform Spectroscopy: A Self-Compensating Label-Free Immunosensor Using Double-layers of Porous SiO2. *Journal of the American Chemical Society.* 2006;128:4250-4252.

32. Pacholski C, Sartor M, Sailor MJ, Cunin F, Miskelly GM. Biosensing using porous silicon double-layer interferometers: reflective interferometric Fourier transform spectroscopy. *Journal of the American Chemical Society.* 2005;127(33):11636-11645.
33. Jane A, Dronov R, Hodges A, Voelcker NH. Porous silicon biosensors on the advance. *Trends in Biotechnology.* Apr 2009;27(4):230-239.
34. De Stefano L, Arcari P, Lamberti A, et al. DNA optical detection based on porous silicon technology: from biosensors to biochips. *Sensors.* Feb 2007;7(2):214-221.
35. Jane AO, Szili EJ, Reed JH, Gordon TP, Voelcker NH. Porous silicon biosensor for the detection of autoimmune diseases2007.
36. Urmann K, Walter J-G, Scheper T, Segal E. Label-Free Optical Biosensors Based on Aptamer-Functionalized Porous Silicon Scaffolds. *Analytical Chemistry.* 2015;87(3):1999-2006.
37. Urmann K, Arshavsky-Graham S, Walter JG, Scheper T, Segal E. Whole-cell detection of live lactobacillus acidophilus on aptamer-decorated porous silicon biosensors. *Analyst.* 2016.
38. Yoo L, Ahn K-Y, Ahn J-Y, et al. A simple one-step assay platform based on fluorescence quenching of macroporous silicon. *Biosensors and Bioelectronics.* 3/15/ 2013;41(0):477-483.
39. Terracciano M, De Stefano L, Borbone N, et al. Solid phase synthesis of a thrombin binding aptamer on macroporous silica for label free optical quantification of thrombin. *RSC Advances.* 2016;6(90):86762-86769.
40. Stoltenburg R, Schubert T, Strehlitz B. In vitro Selection and Interaction Studies of a DNA Aptamer Targeting Protein A. *PLoS ONE.* 2015;10(7):e0134403.
41. Shtenberg G, Massad-Ivanir N, Engin S, Sharon M, Fruk L, Segal E. DNA-directed immobilization of horseradish peroxidase onto porous SiO2optical transducers. *Nanoscale Res Lett.* 2012;7(1):443.
42. Massad-Ivanir N, Shtenberg G, Zeidman T, Segal E. Construction and Characterization of Porous SiO(2)/Hydrogel Hybrids as Optical Biosensors for Rapid Detection of Bacteria. *Advanced Functional Materials.* Jul 23 2010;20(14):2269-2277.
43. Segal E, Perelman LA, Cunin F, et al. Confinement of thermoresponsive hydrogels in nanostructured porous silicon dioxide templates. *Advanced Functional Materials.* May 2007;17(7):1153-1162.
44. Protein and DNA Size Calculator. 2012; http://www.calctool.org/CALC/prof/bio. Accessed 01.09.2012.
45. Walter JG, KÃ¶kpinar Ã, Friehs K, Stahl F, Scheper T. Systematic investigation of optimal aptamer immobilization for protein-microarray applications. *Analytical Chemistry.* 2008;80(19):7372-7378.
46. Walter J-G, Heilkenbrinker A, Austerjost J, Stahl F, Scheper T. Aptasensors for Small Molecule Detection. *Z. Naturforsch.* 2012;67b:976-986.
47. Song SP, Wang LH, Li J, Zhao JL, Fan CH. Aptamer-based biosensors. *Trac-Trends in Analytical Chemistry.* Feb 2008;27(2):108-117.
48. Markham NR, Zuker M. UNAFold. Vol 4532008:3-31.
49. Hill AV. PROCEEDINGS OF THE PHYSIOLOGICAL SOCIETY: January 22, 1910. *The Journal of Physiology.* 1910;40(suppl):i-vii.

50. Kurganov BI, Lobanov AV, Borisov IA, Reshetilov AN. Criterion for Hill equation validity for description of biosensor calibration curves. *Analytica Chimica Acta.* 2001;427(1):11-19.
51. Moks T, Abrahmsén L, Nilsson B, Hellman U, Sjöquist J, Uhlén M. Staphylococcal protein A consists of five IgG-binding domains. *European Journal of Biochemistry.* 1986;156(3):637-643.
52. Jing M, Bowser MT. A Review of Methods for Measuring Aptamer-ProteinEquilibria. *Analytica chimica acta.* 11/10 2011;686(1-2):9-18.
53. Urmann K, Modrejewski J, Scheper T, Walter Johanna G. Aptamer-modified nanomaterials: principles and applications. *BioNanoMaterials.* Vol 02016.
54. Chang AL, McKeague M, Smolke CD. Facile characterization of aptamer kinetic and equilibrium binding properties using surface plasmon resonance. *Methods in enzymology.* 2014;549:451-466.
55. Chang AL, McKeague M, Liang JC, Smolke CD. Kinetic and equilibrium binding characterization of aptamers to small molecules using a label-free, sensitive, and scalable platform. *Anal Chem.* Apr 1 2014;86(7):3273-3278.
56. Tellinghuisen J. Statistical Error Propagation. *J. Phys. Chem. A.* 2001;105:3917-3921.
57. Mariani S, Strambini LM, Barillaro G. Femtomole Detection of Proteins Using a Label-Free Nanostructured Porous Silicon Interferometer for Perspective Ultrasensitive Biosensing. *Anal Chem.* Aug 22 2016.
58. Pacholski C, Yu C, Miskelly GM, Godin D, Sailor MJ. Reflective Interferometric Fourier Transform Spectroscopy: A Self-Compensating Label-Free Immunosensor Using Double-Layers of Porous SiO2. *Journal of the American Chemical Society.* 2006/04/01 2006;128(13):4250-4252.
59. Demirel G, Çağlayan MO, Garipcan B, Duman M, Pişkin E. Oriented immobilization of IgG on hydroxylated Si(001) surfaces via protein-A by a multiple-step process based on a self-assembly approach. *Journal of Materials Science.* 2007;42(22):9402-9408.
60. Li J, Sailor MJ. Synthesis and characterization of a stable, label-free optical biosensor from TiO2-coated porous silicon. *Biosensors and Bioelectronics.* 5/15/ 2014;55:372-378.
61. Chang TC, Huang SH. Evaluation of Coagulase Activity and Protein A Production for the Identification of Staphylococcus aureus. *Journal of Food Protection.* // 1995;58(8):858-862.

Figure 1. A: Schematic illustration of the experimental setup, depicting instrumentation and flow-cell configuration. The lower panels show HRSEM micrographs of porous silicon nanostructures (left) and schematics of aptamer-functionalized $PSiO_2$ before and after target capture (right). **B:** Reflectivity collection and processing steps. Reflectivity spectra were recorded (1) and a Fast Fourier transformation was applied (2). The signal was then expressed as the relative change in EOT over the course of the experiment (3). The final biosensing result was extracted as the relative change in EOT before and after exposure of the aptamer-functionalized $PSiO_2$ scaffold to the sample solution (3).

Figure 2: Relative change in EOT vs. time of PAA-functionalized $PSiO_2$ during a typical biosensing experiment. A baseline was acquired in SB followed by introduction of PA (trace a) or IgG (trace b), respectively. After rinsing to remove unbound molecules, a stable readout signal was attained. Note that during buffer exchange and rinsing, EOT measurements were briefly paused.

Figure 3: Averaged optical response (relative EOT) of N_{40}-functionalized $PSiO_2$ and PAA-functionalized $PSiO_2$ upon exposure to IgG or PA at a concentration of 5 µM ($n > 3$ for each experiment). * indicates statistically significant difference between the values (t-test, $p < 0.05$).

Figure 4: Aptamer-functionalized $PSiO_2$ biosensor responses, expressed as the relative EOT change, from different concentrations of PA (triangles) and IgG (circles). The solid line is a fit using equation (1), and K_D is determined, yielding 14 ± 1 µM.

Figure 5: a) Relative change in EOT vs. time of PAA-functionalized $PSiO_2$ upon exposure to a concentration of 1 µM of PA (below the LoD) followed by incubation with IgG at the same concentration and a final rinsing step with SB. b) Optical response of the PAA-biosensor upon introduction of 1 µM IgG without prior incubation with PA.

Figure 6: Sensitivity enhancement of the PAA-functionalized $PSiO_2$ biosensor. Averaged optical response (relative EOT) of the biosensor upon exposure to 1 µM of: PA, IgG or both in a successive manner. Schematic illustration of biomolecules captured by the aptamers within the porous scaffold. Upper dashed line indicates the LoD value. Differences between both single exposures (of PA or IgG) and the sandwich assay are statistically significant ($p<0.05$, $n\geq3$).

Figure 1.

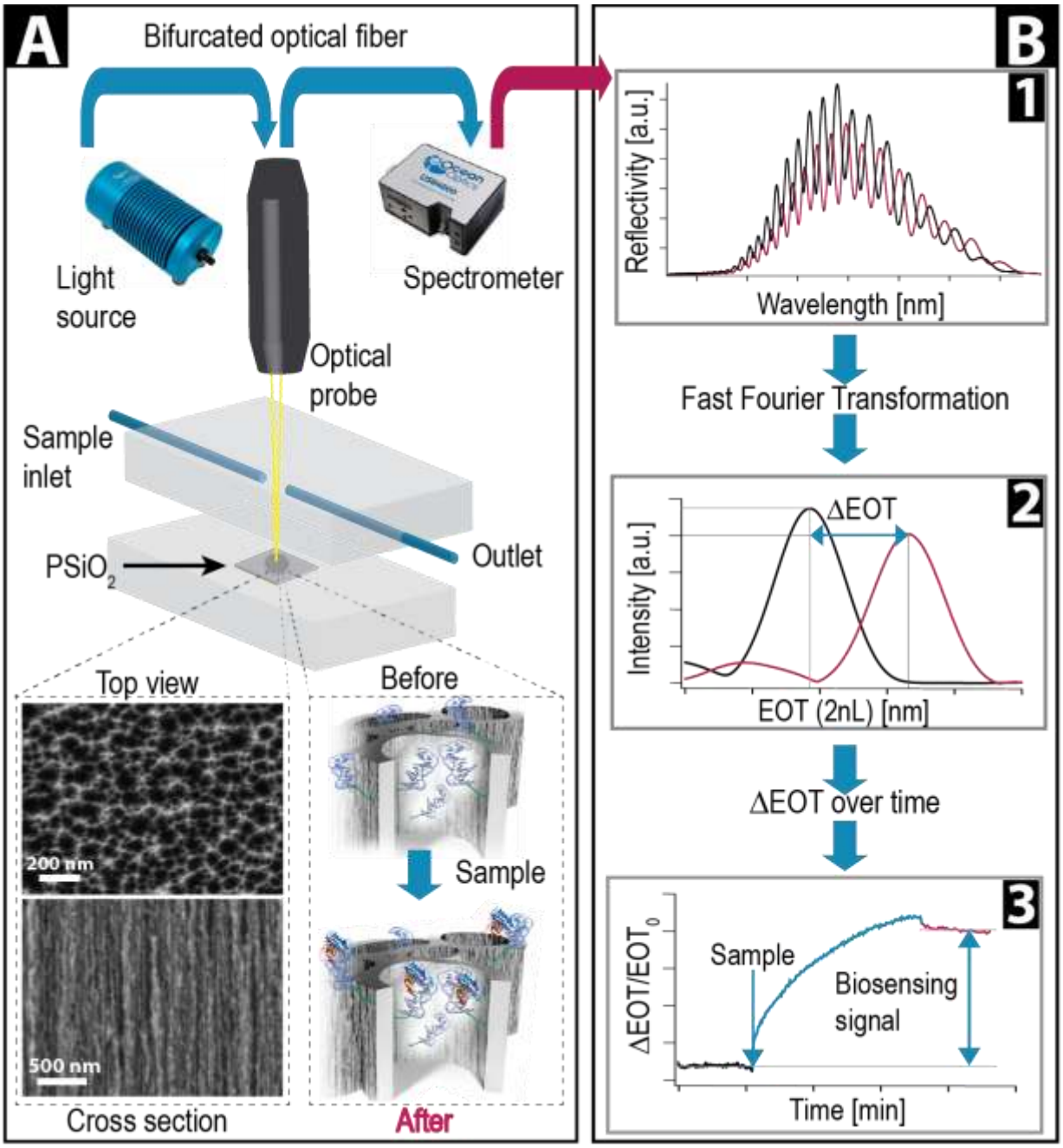

Figure 2.

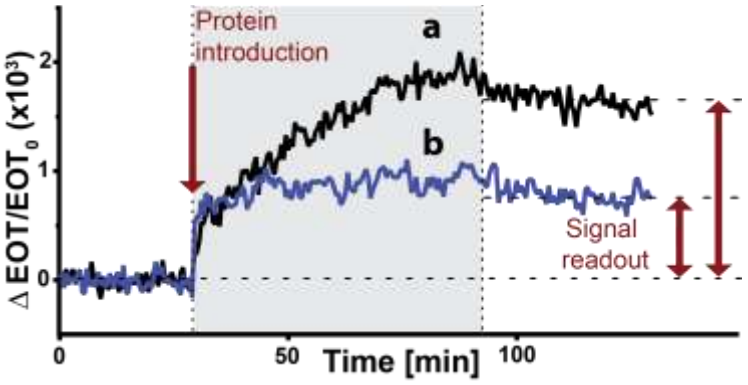

Figure 3.

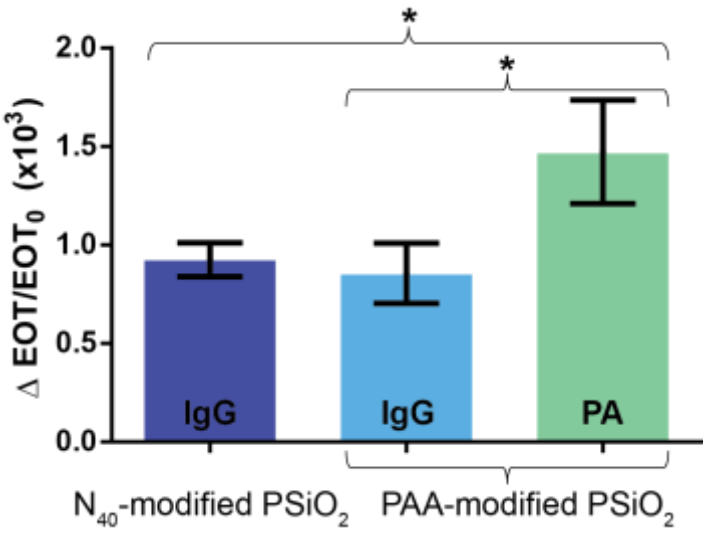

Figure 4.

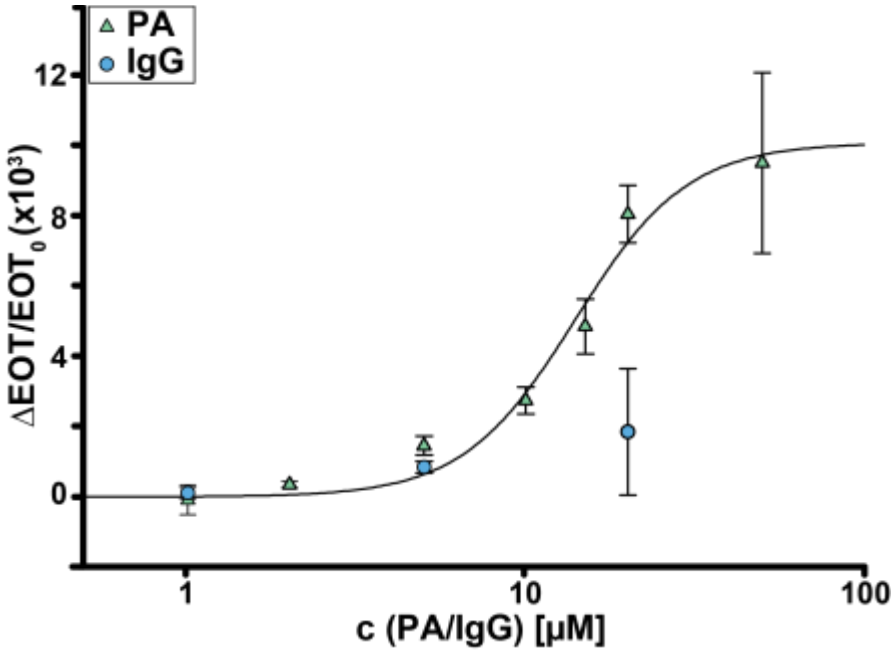

Figure 5.

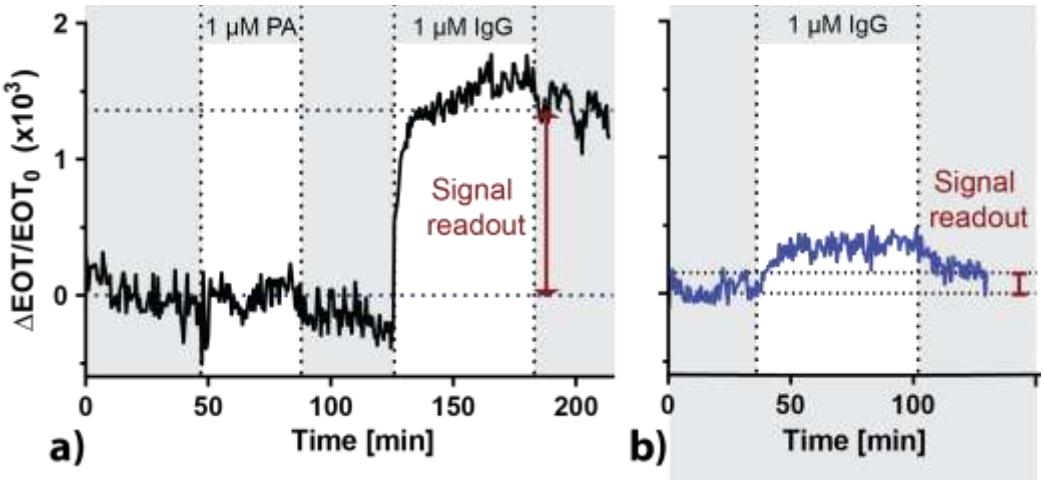

Figure 6.